The Meteoritical Society

Meteoritics & Planetary Science 44, Nr 10, 1465–1474 (2009)
Abstract available online at http://meteoritics.org

Capture effects in carbonaceous material: A Stardust analogue study

Marc FRIES[1*], Mark BURCHELL[2], Anton KEARSLEY[3], and Andrew STEELE[4]

[1]NASA Jet Propulsion Laboratory, 4800 Oak Grove Dr. MS 183-301, Pasadena, California 91109, USA
[2]School of Physical Sciences, University of Kent, Canterbury CT2 7NH, UK
[3]Department of Mineralogy, Natural History Museum, London SW7 5BD, UK
[4]Geophysical Laboratory, Carnegie Institution of Washington, 5251 Broad Branch Rd. NW, Washington, D.C. 20001, USA
[*]Corresponding author. E-mail: marc.d.fries@jpl.nasa.gov

(Received 11 March 2009; revision accepted 28 August 2009)

Abstract–It is reasonable to expect that cometary samples returned to Earth by the Stardust space probe have been altered to some degree during capture in aerogel at 6.1 km/s. In order to help interpret the measured structure of these particles with respect to their original cometary nature, a series of coal samples of known structure and chemical composition was fired into aerogel at Stardust capture velocity. This portion of the study analyzed the surfaces of aerogel-embedded particles using Raman spectroscopy. Results show that particle surfaces are largely homogenized during capture regardless of metamorphic grade or chemical composition, apparently to include a devolatilization step during capture processing. This provides a possible mechanism for alteration of some aliphatic compound-rich phases through devolatilization of cometary carbonaceous material followed by re-condensation within the particle. Results also show that the possibility of alteration must be considered for any particular Stardust grain, as examples of both graphitization and amorphization are found in the coal samples. It is evident that Raman G band (~1580 cm^{-1}) parameters provide a means of characterizing Stardust carbonaceous material to include identifying those grains which have been subjected to significant capture alteration.

INTRODUCTION

The study of Stardust samples is complicated by the fact that Stardust samples have experienced some degree of processing during aerogel capture at 6.1 km s^{-1}. Because of this, describing native cometary carbonaceous materials from measurements of the structure and chemistry of Stardust samples requires a series of assumptions about the nature and extent of capture alteration. The research presented here is intended to assist that process by using a series of coal samples of known structure and chemistry to describe changes they undergo during hypervelocity aerogel capture. The results of this work will be used to help describe alteration of Stardust carbonaceous materials on capture and from there draw conclusions about the state of native 81P/Wild 2 materials. Previous work has been done on capture alteration using analogue Allende particles fired into aerogel (Flynn et al. 2006; Hoppe et al. 2006), but the carbonaceous component of these samples was sequestered within other mineral phases. This work will investigate more fundamental aspects of the alteration of carbonaceous material free from other,complicating influences such as the mechanical behavior of a silicate component. As a consequence, this work differs from direct studies of Stardust materials in terms of both target composition and particle size. To date, no purely carbonaceous Stardust particles have been found and so this study is not intended to be a direct comparison with known Stardust materials. Additionally, because of the necessity to minimize the effect of laser heating during Raman analysis, measurements collected in this study were restricted to particles ~5 μm in diameter (i.e., large relative to the 1 μm Raman excitation spot) which are large compared to typical carbonaceous phases in Stardust particles. By examining and characterizing the effects of capture on carbonaceous matter absent other effects, we gain two important pieces of insight. For one, the degree of capture alteration of a given particle can be better understood so as to better separate native cometary features from capture effects, and secondly, conclusions can be drawn on the native state of Stardust examples that have demonstrably experienced capture alteration.

Stardust Carbonaceous Materials

Carbonaceous materials have long been identified as components of cometary bodies based on astronomical

observations of active comets (i.e., review by Irvine [1998]) and on spectroscopic measurements during spacecraft flybys of active comets. It was no surprise, then, that investigation of particles from comet 81P/Wild 2 returned to Earth by the Stardust mission (Brownlee et al. 2006) shows that carbonaceous materials are a relatively common constituent (Sandford et al. 2006). Carbonaceous materials in Stardust particles are of particular scientific interest, as they not only serve as indicators of the pre-accretion gas-phase chemistry of cometary material formation, but also as sensitive indicators of alteration during accretion and parent body alteration. These materials are found spanning a surprisingly wide range of composition, chemistry, and structure. Initial studies of Stardust particles showed the presence of a condensed component heterogeneous in terms of N/C and O/C content ratios, distribution among particles, and chemical functionality (Sandford et al. 2006). A labile, aliphatic compound-rich component was also noted (McKeegan et al. 2006; Sandford et al. 2006; De Gregorio et al. 2009). Generally speaking, carbonaceous materials identified in 81 P/Wild 2 samples include a condensed macromolecular carbonaceous phase of heterogeneous structure (Keller et al. 2006; Sandford et al. 2006) and include some materials that are considerably more N-rich than that of carbonaceous chondrites (Cody et al. 2008). Recently, De Gregorio et al. (2009) offered a breakdown of Stardust carbonaceous phases into five types: 1) rare "cometary organic globules" similar to nanoglobules noted in the Tagish Lake meteorite (Nakamura-Messenger et al. 2006) and elsewhere, 2) "nitrogen-rich cometary organics" described based on chemistry alone, 3) organics with associated oxide and/or sulfide nanoparticles, 4) organics found within aerogel and believed to be cometary based on nitrogen isotopes, and 5) the labile organic phase noted above. The characterization and description of Stardust carbonaceous phases is an evolving work, but it is worth noting that the phases described above are susceptible to or are themselves products of capture alteration. Carbonaceous material dispersed in aerogel proximal to a capture track are the product of evaporation from the captured particle, condensed carbonaceous matter dispersed through cometary grains may be residue which survived devolatilization, and the labile phase is especially susceptible to evaporation. Another important point is that, even in the absence of capture alteration, it is apparent that Stardust carbonaceous phases are diverse in terms of structure, chemistry, and isotopic composition. In order to thoroughly describe the state of carbonaceous phases on the 81P/Wild 2 parent body, it is necessary to thoroughly understand Stardust particles as the products of highly stochastic capture processing and separate the native features from the imposed.

Stardust Aerogel

Aerogel is a highly porous, transparent form of SiO_2, whose under-dense nature permits relatively intact capture of high speed particles (a review of capture in aerogel is given in Burchell et al. 2006). Capture of 81 P/Wild 2 cometary particles occurred at around 6.1 km/s into aerogel which was designed to be density graded, i.e., density of 5 kg m^{-3} at the front face rising to 50 kg m^{-3} at the rear of the 3 cm deep blocks (Tsou et al. 2003). Burchell et al. (2009) have suggested an analysis of the tracks in the Stardust aerogel implies the aerogel on average behaved as if it had a mean density of just under 20 kg m^{-3}. Trigo-Rodríguez et al. (2008) estimate peak shock pressures during capture in aerogel of 20 kg m^{-3} of just under 1 GPa. In its rapidity and thermal effects, aerogel capture amounts to shock processing and may have the dual effects of affecting both structure (via amorphization) and composition (via devolatilization) of cometary carbonaceous materials.

During capture, a heat pulse is delivered to the particle that can cause melting and ablation. Based on observing mineralogical changes in captured grains in laboratory experiments, Noguchi et al. (2007) estimated that during capture in aerogel of density 30 kg m^{-3} at 6.2 km s^{-1}, a heat pulse is delivered to the captured grain which raises its surface temperature to 500–600 °C for of order 1 μs. In separate experiments, Burchell et al. (2009) show that even capture in aerogel (density 25 kg m^{-3}) at the lower speed of 3.1 km s^{-1} is sufficient to melt and ablate the surface of a stainless steel projectile (melting point 1400 °C), and Hörz et al. (2008, 2009) show that capture in 20 kg m^{-3} aerogel at 6 km s^{-1}, is sufficient to melt the surface of Al_2O_3 spheres (melting point 2054 °C). Modelling suggests that a molten aerogel wrapping forms during capture, with a peak temperature of some 2100 °C for time scales of order 0.1 ms (Roskosz et al. 2008). The captured particles themselves show disaggregation and some size sorting (Brownlee et al. 2006) and any fragments shed by a particle during capture (and which end up lining the wall of the aerogel track) will also undergo heating whilst embedded in the molten aerogel of the track wall. Due to steep thermal gradients, interiors of particles more than a few μm across will not experience significant heating above a few hundred °C. Surviving tochilinite in hypervelocity experiments using Murchison meteorite powder indicate grain interior temperatures did not exceed 300 °C (Noguchi 2007). Other researchers (Berger 2008) indicate that the interior temperature in Stardust samples did not exceed 340 °C as suggested by survival of pyrrhotite. There is thus clear evidence that while the surface of particles can undergo a significant degree of thermal processing during capture, the overall picture of particle capture is one of high temperatures generated over small spatial scales and inhomogeneously distributed to the captured particles.

It was shown by Burchell et al. (2001, 2006) that Raman analysis (carried out in-situ) could identify mineral grains captured in aerogel. Later this was extended to identifying

Table 1. Composition and metamorphic grade (coal rank) of the coals used in this experiment.

		Coal sample rank and composition				
	Coal rank	%C (wt)	O/C	H/C	N/C	S/C
Graphite powder	n/a	100	–	–	–	–
PSOC 1468	Anthracite (an)	88.85	0.02	0.01	0.01	0.01
DECS 21	Anthracite (an)	80.26	0.05	0.04	0.01	0.01
DECS 31	High volatile A bituminous (hvAb)	76.32	0.08	0.06	0.02	0.01
DECS 24	High volatile C bituminous (hvCb)	66.05	0.14	0.07	0.02	0.08
PSOC 1534	Subbituminous C	63.06	0.32	0.08	0.01	0.00

some specific organic grains (polymethylmethacrylate and polyethylmethacrylate) captured in aerogel (Burchell et al. 2004). The D and G carbon bands can also be identified in carbon-rich particles captured in aerogel (e.g., see Burchell et al. 2006b for examples using grains of Murchison and Allende meteorites). However, Foster et al. (2007) reported that there were shifts in the mean peak position and width of the carbon D and G bands in some meteorite samples after capture in aerogel, indicating effects due to capture. Raman analysis of aromatic organics (characterized by observation of the carbon D and G bands) contained in 81P/Wild 2 dust grains was carried out (Sandford et al. 2006; Rotundi et al. 2008) and early results showed that Raman spectral features of Stardust particles populate a broad range of values similar to those for interplanetary dust grains (IDPs) and primitive meteorites. A new method has been proposed for calculation of effective metamorphic temperature of the parent body based on Raman and NMR spectral features (Cody et al. 2008). This will be useful for describing the thermal history of the 81P/Wild 2 parent body, but before it can be applied accurately we must first address the degree to which Stardust capture processing has altered the captured material.

We present here the results of an analogue study on hypervelocity capture of a range of coal samples of known chemistry and structure in analogue aerogel targets. The resulting Raman spectra provide an initial measure of alteration in carbonaceous materials due to capture processing and the implications of this for the 81P/Wild 2 dust samples are considered.

METHOD

Samples of coal were fired into aerogel targets at velocities of around 6 km/s in order to simulate the capture dynamics of 81 P/Wild 2 cometary particles upon capture by the Stardust spacecraft. The coal samples are standardized examples purchased from the U.S. Department of Energy Coal Sample (DECS) Bank and Database. These standard coal libraries have been extensively analyzed using ASTM standardized methods (ASTM Standard D3172-07a 2007 and related standards) and are accessible by the public. Five coal samples and a commercially available, high purity graphite powder were selected to represent a broad range of metamorphic grade in and, to a lesser degree, a range of heteroatom (hydrogen, oxygen, nitrogen, and sulfur) contents. For the purposes of this paper, all six samples will be referred to as "coal"; see Table 1. This range of values was chosen to simulate as closely as possible the wide range of structure and heteroatom content observed in Stardust samples (Sandford et al. 2006).

Carbon samples were fired into aerogel targets using the light gas gun at the Hypervelocity Impact Laboratory at the University of Kent (Burchell et al. 1999). The gun fires projectiles loaded in a sabot which is discarded in flight. Thus multiple small grains can be fired at similar speed in a single shot. The impact speed was determined using a combination of sensors along the flight path and is accurate to typically 2%. Homogenous silica aerogel targets of 30 ± 2.4 mg/cm^3 were used as targets (similar to those described in Noguchi et al. 2007), along with a single example of density-gradient, Stardust "flight-type" aerogel (manufactured as described in Jones 2007). All six carbon-bearing materials were fired into homogenous aerogel at 6.15 ± 0.1 km/s under vacuum, and a sample of the anthracite coal PSOC 1468 was fired into "flight-type" aerogel at 6.13 km/s. This portion of the experiment was done to test the hypothesis that homogenous higher density aerogel would result in measurably different carbonaceous material structure due to more rapid deceleration. Since Raman measurements were performed on particles in their insulating aerogel medium, particles larger than ~5 microns in diameter (i.e., large relative to the ~1 μm laser spot diameter) were selected for analysis to reduce the likelihood of thermal alteration by the excitation beam.

Raman spectra were collected of both as-received coal powders and of coal particles embedded in target aerogel (Fig. 1). Aerogel blocks were split along the long axis of particle tracks using a sterile blade and the tracks were then inspected along their length using reflected and transmission optical microscopy to identify target particles. Spectra were collected using a JASCO NRS^{-3}100 Raman spectrometer with 532 nm wavelength laser excitation. Laser power was measured at the focal plane and restricted to 0.041 mW total power over a spot ~1 micron in diameter, for a power density of ~5,200 W/cm^2. Power limiting is done with an OD 2 optical density filter in the excitation beam path. Previous work with sub-micron, shear-damaged troilite particles on gold foil showed that 0.033 mW power over a 360 nm diameter spot (~32,000 W/cm^2) could be used without

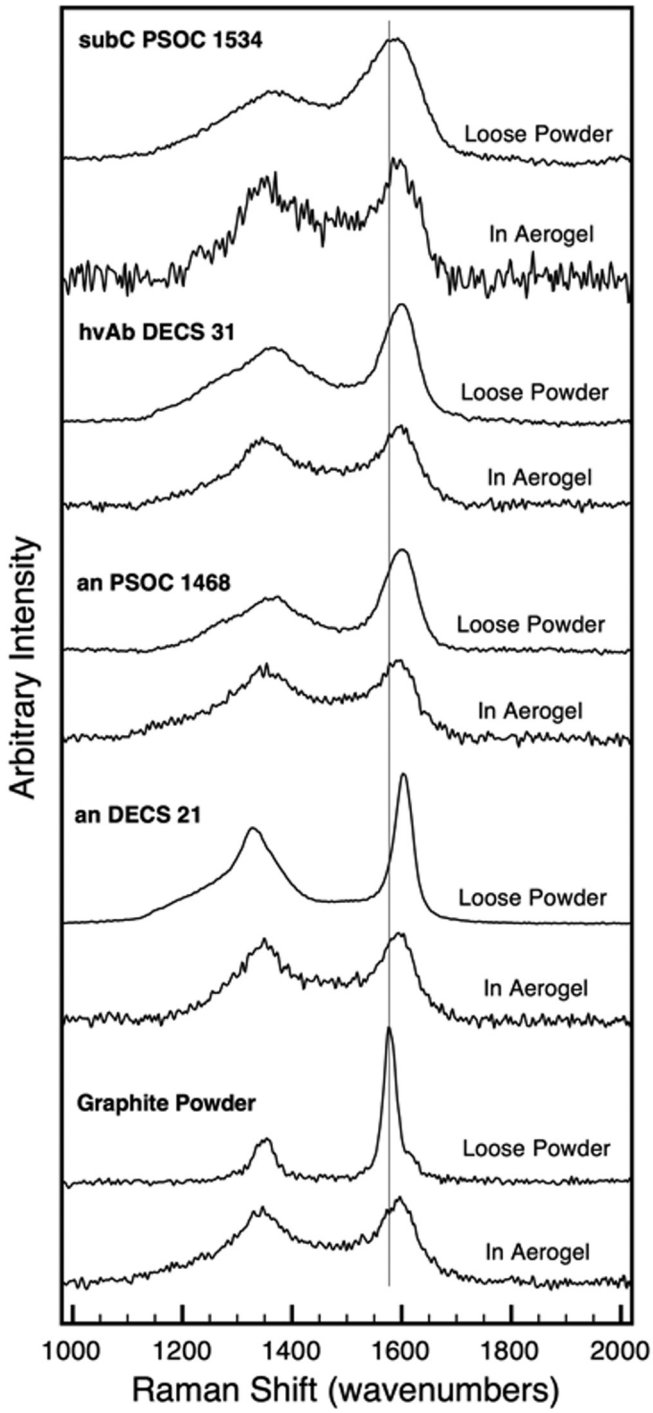

Fig. 1. Raman spectra comparison. "Before and after" spectra of each coal sample and a selected spectrum of the same material embedded in aerogel. The gray vertical line is fixed at 1580 cm^{-1} for reference. Note the similar appearance of the aerogel-embedded spectra.

oxidizing to magnetite under air. This is used as a standard here for analysis of Stardust samples, with the goal of restricting laser power such that fine, shocked sulfides in captured particles are protected from laser damage. The theory is that sulfides are the most sensitive mineral indicators of laser damage and so laser heating damage should be minimized or eliminated for the particle by restricting laser power to less than that which damages sulfides. One coal particle captured in aerogel was used as a test subject to test for laser damage in aerogel-embedded particles. Raman spectra were collected for 420 s with 6 s integrations with no measurable change in spectra over the full duration of the measurement. All spectra were collected with ~5,200 W/cm^2 power density (i.e., ~1/6 the power identified as a lower limit for particles on gold foil), 3 s integration time for 20 accumulations (60 s total collection time) and a 100× objective lens. No overt indications of laser damage (dramatically different spectra over the course of a measurement, changes in background fluorescence, changes in Raman peak position and/or width during measurement, or visible damage after the measurement) were noted in the course of the analyses described here.

All Raman spectra collected were treated using spline background subtraction and Gaussian peak deconvolution using the Multipeak Fitting package of Igor 6.04 spectral analysis software. Only the carbon G band parameters are discussed here. While both the G and D bands have been shown to follow trends based on crystalline order (Tuinstra and Koenig 1970; Pasteris and Wopenka 1993), additional complexity is found in the D band. The actual origin of the D band is somewhat controversial and it displays the unusual property of shifting its spectral position with change in excitation wavelength (Matthews 1999; Sood 2001) which indicates that it is not solely a Raman mode. Determination of the D band position is also complicated by degeneration into a non-Gaussian profile in even moderately amorphous samples (note D band shapes in Fig. 1, and especially compare DECS 31 to DECS 21). By contrast, the G band is a "pure" Raman mode, its analysis is straightforward, and trends in G band parameters are clearly seen versus crystalline order (open symbols in Fig. 2). Additionally, materials that feature crystalline domains that are large with respect to the Raman analysis spot occupy their own region of a G band center versus G band width graph (note the "Graphite" region in Fig. 2). This allows for relatively simple and definitive recognition of very well ordered materials.

Raman data of PSOC 1468 in both homogenous and flight-type aerogels produced one apparent outlier value each (Fig. 3). Each value was tested using Dixon's Q significance test using vector values from the mean to incorporate both G band position and width in the calculation. The homogenous aerogel outlier failed with Q = 0.83 and the flight-type outlier failed with Q = 0.86 versus Q_{CRIT} = 0.72 (P = 0.05). These outliers are due to actual physical effects of graphitization (homogenous aerogel example) and amorphization (flight-type example). Their appearance is not surprising considering the stochastic nature of shock effects, but they are rejected from calculating the G band mean values on the logical basis that the point of the measurement was to compare typical alteration products of capture and not rarer, extreme examples.

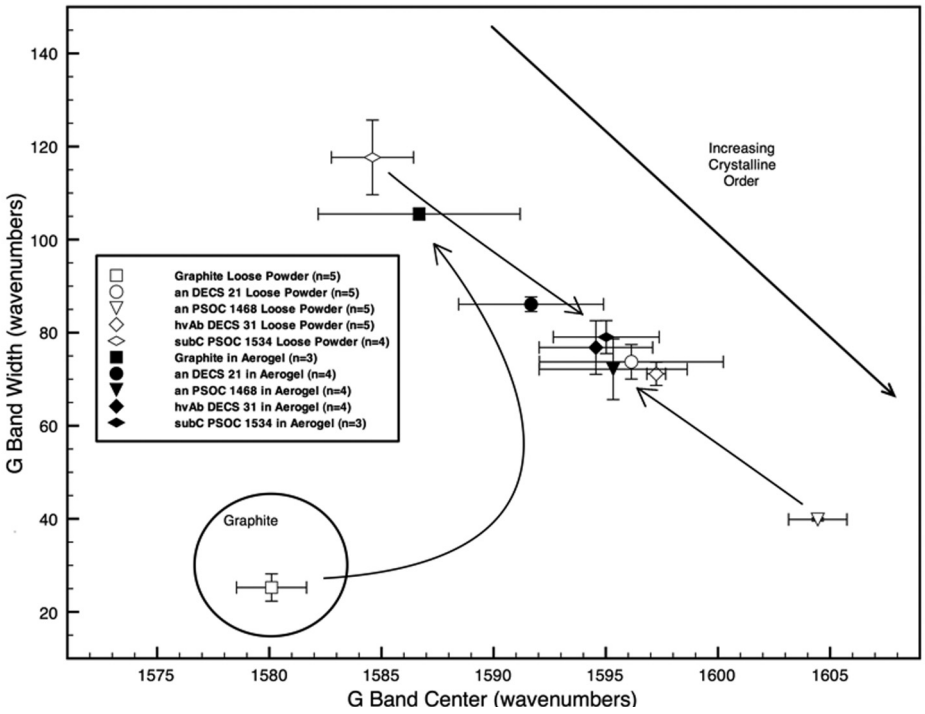

Fig. 2. Raman G band parameters derived from Gaussian fits. Open symbols indicate as-received coal and filled symbols show the same coal after capture by homogenous aerogel at ~6 km s^{-1}. The large circle in the lower left shows the approximate G band parameters for crystalline graphite. Note the trend in as-received coal from upper left to lower right, defining a trendline of increasing crystalline order and thermal maturity towards the lower right. Note how coal fired into aerogel tends to "swap ends" on the graph. Graphite is strongly amorphized while the poorly ordered PSOC 1534 has become more ordered. Crystalline graphite does not withstand the physical shock of capture well, while disordered carbon undergoes significant ordering (see text).

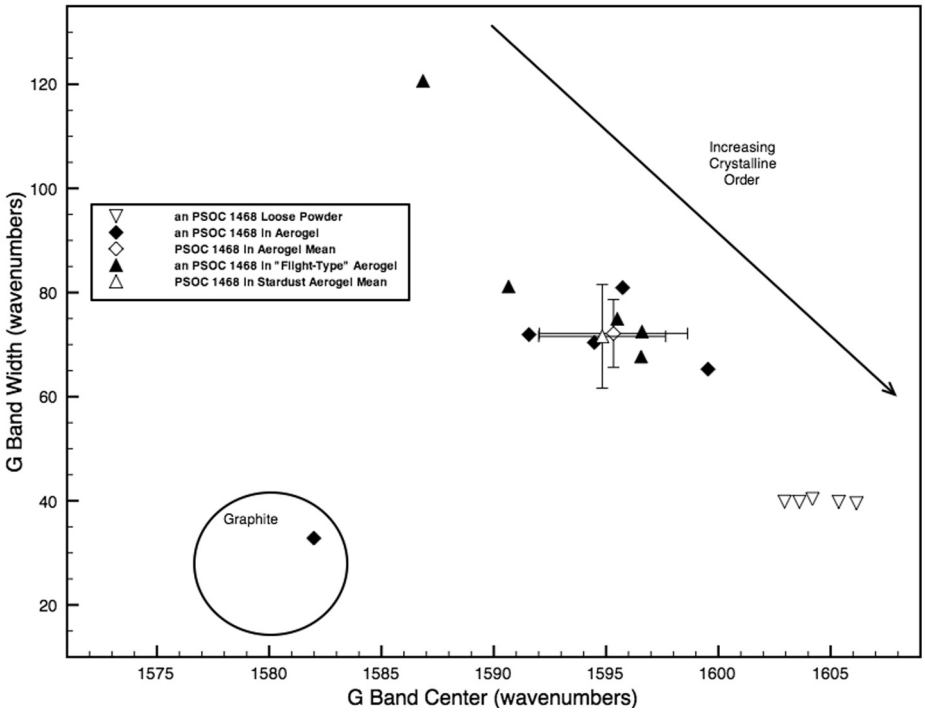

Fig. 3. Comparison between capture in homogenous aerogel versus capture in density gradient, "flight-type" aerogel. Both examples produce an outlier value, with one instance of graphitization in homogenous aerogel and one instance of strong amorphization in flight-type aerogel. Disregarding these outliers, the statistical difference between the two mean values is insignificant. Error bars represent 1σ.

RESULTS AND DISCUSSION

Homogenous Aerogel Tests

All samples produced at least three particles suitable for Raman analysis, with the exception of hvCb DECS 24 which generated neither large tracks nor embedded particles greater than the 5 micrometers in diameter used as a lower size limit in this experiment. DECS 24 is a high volatile coal, but this by itself does not explain the lack of consolidated debris since the high volatile coal subC PSOC 1534 features a similar overall carbon content in a less-ordered coal but usable particles survived capture. DECS 24 features the highest S/C ratio of all the coal samples (0.08). ASTM-standard proximate analysis shows that about 50% of the sulfur in DECS 24 is bound within the carbonaceous component (2.64% by weight pyritic, 0.5% sulfate, 2.64% organic in dry analysis). A possible explanation for the complete dissociation of this coal is that the sulfur bound up in carbonaceous matter forms a large number of substitution point defects in the crystalline structure, providing nuclei for failure during shock. This might cause fragmentation and loss during the shot, or if the absence of larger debris within the tracks is a function of processing during aerogel capture, the implication is that survival of carbonaceous particles in Stardust samples could be biased towards relatively sulfur-poor original materials. As this observation is based upon only a single experimental shot, we suggest that further experimental work on such sulfur-rich materials is needed to confirm our initial results, to document the survivability of grains, and the mechanisms of their destruction. However, as we discuss later in this paper, it is also possible that Wild 2 organic-rich materials within grains dominated by inorganic minerals may also have been shielded from, or conversely subjected to, more intense localized shock effects. Here the style of "mechanical" alteration may differ, and sulfur-rich organic matter may behave differently. The lack of surviving particles of sufficient size for our analytical protocol means that DECS 24 is not available for analysis of Raman spectral change in this study.

The results from capture in homogenous aerogel show a surprising trend. Figure 2 shows average values for all coal samples both as loose powder and as small particles embedded in aerogel. There is a tendency for the materials to "swap ends" on this graph after capture in aerogel, with similar G band parameters indicating a general homogenization of carbonaceous material ordering. Out of all the samples, the graphite powder is the most strongly amorphized during capture. PSOC 1468 anthracite, the most strongly ordered of the coals, features a pronounced shift to less order following capture. The poorly ordered sub-bituminous C coal PSOC 1534 exhibits a marked increase in crystalline order following capture, and in general the various coals trend towards the mid-point in the crystalline ordering trend during capture. Captured particles (excepting graphite powder) exhibit G band center and width values of 1593.3 ± 4.2 and 75.6 ± 13.2, respectively. Relatively low-toughness graphite is strongly amorphized during capture. The same is true (to a lesser degree) for the low-volatile anthracite PSOC 1468, while the high-volatile anthracite DECS 21 also amorphized but to a smaller degree. The trend of alteration most closely reflects initial structure, with the degree of amorphization during capture being proportional to initial crystallinity. In looking at coals that are less thermally mature, the high volatile bituminous coal DECS 31 showed very slight disordering while the thermally immature, volatile-rich sub-bituminous PSOC 1534 exhibited marked graphitization. Considerable literature exists on the vagaries of graphitization (i.e., Fischbach 1963; Murty 1969a; Murty 1969b; Crespo and Pradell 1996), and it is known that higher heteroatom content slows graphitization rate, presumably through restriction of graphitic crystallite growth due to grain boundary pinning by localized heteroatom enrichment (Beyssac et al. 2003). Therefore, graphitization in nature must be accompanied by devolatilization in order to proceed, but conversion to crystalline graphite is not necessarily possible. This implies that the graphitization of PSOC 1534 requires devolatilization during capture. The primary explanation for capture alteration in this study is that it is essentially a very rapid form of graphitization of organic solids seen elsewhere in nature, featuring paired devolatilization and graphitization to a more ordered final form. Overall, results indicate that carbon crystallinity is not randomized during capture shock processing, nor are all materials either uniformly amorphized by shock or graphitized by residual heat immediately following capture. That the final product is consistent largely regardless of coal type implies that devolatilization occurs as well since the presence of heteroatoms serves to retard crystallization in carbonaceous materials, which means that the final product should preserve the original (but distorted) trend line if the heteroatom contents were not driven to similar values during capture. Raman analyses on opaque coal materials are restricted to a small fraction of a micrometer in depth so the measurements performed here are well within a severely altered surface layer in the captured particles. Given these restraints, it is likely that the material analyzed using Raman spectroscopy (i.e., a thin layer at the particle surface) has been devolatilized during capture. Future work will determine the extent of alteration internal to the captured grains.

Returning to the question of recrystallization and amorphization during capture, an alternative explanation is that all particles are strongly amorphized during capture and are then graphitized to a common degree by post-capture thermal processing. In other words, if we were to somehow obtain an instantaneous Raman spectrum of each particle at the moment of capture, it would reveal a degree of disorder greater than those values seen in Fig. 2 due to shock amorphization. Subsequent thermal processing would graphitize each particle to the final values seen here, and the

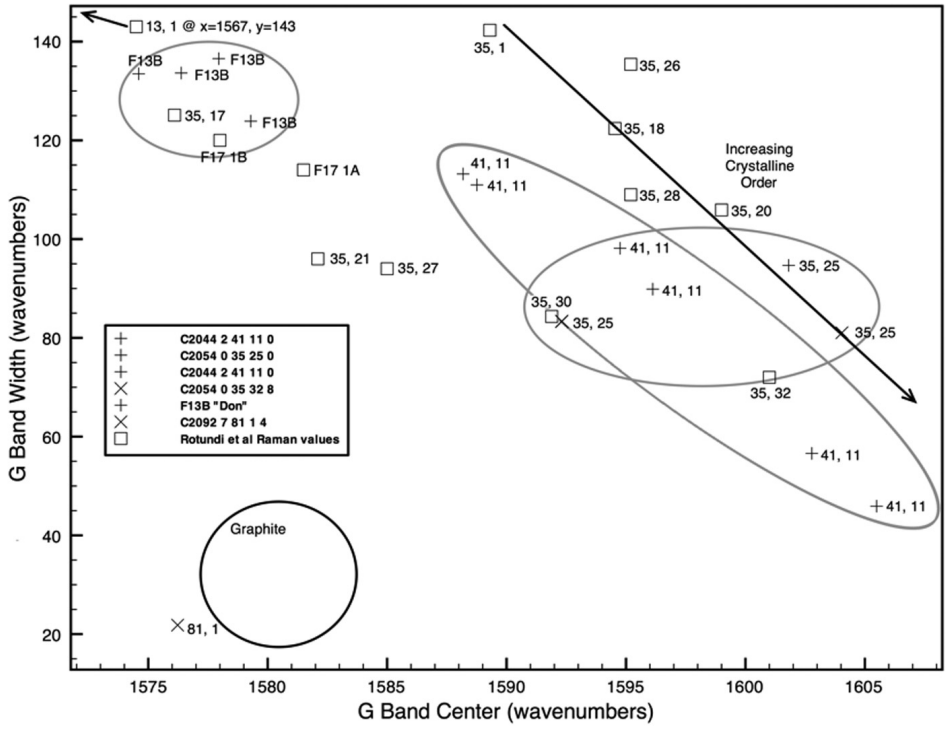

Fig. 4. Raman measurements from selected Raman particles. Square symbols indicate data from Rotundi et al. (2008), other Stardust samples measured in TEM section are shown with (+) symbols, and Stardust particles measured on gold foil are shown as (x). Data from three individual particles are highlighted with gray ellipses. Trends in Raman data reveal characteristics of the original particles. F13B "Don" is consistently amorphous, 41,11 displays broadly heterogenous structure, and 35,25 shows a range of values that resembles capture-altered coal samples (see text).

principal difference between the various particles is the degree of initial disruption exhibited by each coal. The data imply that this intermediate product would be structurally similar to a devolatilized version of sub-bituminous PSOC 1534 since the degree of graphitization of all materials would have to explain the extent of graphitization of this particular coal. This explanation is not reasonable, since if all captured products were graphitized to a common extent, then the heteroatom-free graphite sample would exhibit the same final structure as the other samples.

A third explanation is that the graphitization effects seen here are at least partially due to shear-induced ordering during capture. The best test of this hypothesis is direct Raman measurement of coal particle interiors. If the structure of the interiors strongly diverges from that seen at the outermost grain margins, then shearing effects play a dominant role in capture alteration. Future work will address this hypothesis through examination of particle interiors.

Capture Using Density-Gradient ("Flight-Type") Aerogel

In order to better compare the results of this experiment to Stardust particles, a sample of PSOC 1468 low-volatile anthracite was fired into density-gradient, "flight-type" aerogel similar to that flown on the Stardust mission (Tsou et al. 2003). Comparison of Raman measurements made on PSOC 1468 captured in homogenous aerogel and captured in flight-type aerogel (Fig. 3) show a statistically insignificant variation between the mean values of the two. The sample means were compared by t test with outliers removed. Values for t for G band center and width means were 0.21 and 0.77, respectively. T_{CRIT} for P = 0.05 and 6 degrees of freedom is 2.45, so the null hypothesis is proven and the two values are statistically indistinct. This indicates that there is no discernible difference between the two aerogel types for the purpose of this experiment.

Of special interest is the appearance of a single grain of highly crystalline graphite found in PSOC 1468 coal captured in homogenous aerogel (Fig. 3), where none was observed in the starting material. Two explanations are possible. For one, PSOC 1468 is a well-ordered anthracite and it is possible that some grains of graphitic material may exist within it. It is questionable as to whether a graphitic grain could survive capture unaltered, however, as the graphite powder tested here was strongly disrupted during capture (Fig. 2). The second, more likely, possibility is that the captured grain crystallized immediately after capture in contact with molten aerogel. This possibility must be considered when analyzing graphite grains found in Stardust materials (see particle 81,1 in Fig. 4).

Application to Stardust Results

Coals were chosen for this study to isolate and study the effects of capture on a range of carbonaceous materials with known structure and chemistry. However, the fate of organic matter within cometary particles may also be influenced by the abundant inorganic mineral phases which may modify the shock effects experienced by associated carbonaceous phases. The grain size of Stardust carbonaceous phases also appears to be smaller than the materials examined in our experiments, and such intergranular carbonaceous material may be subjected to localized amplified strain. At present, the extent of variability induced by these effects within Wild 2 dust grains is unknown, but it is reasonable to say that they are likely to hamper direct comparison between the results collected from coal samples and cometary samples. However, understanding the behavior of carbonaceous materials alone is the first step in understanding the behavior of Stardust particles themselves. The general alteration trends for carbon alone should hold true in both cases, and the competing effects of shock amorphization and thermally driven graphitization immediately following capture can be expected to alter Stardust particles in a similar fashion if not to a similar degree. This underlines the need to perform Raman analyses of multiple carbonaceous targets within a single track in order to ascertain trends in the data (see Fig. 4). From there, the emergence of a generalized trend in carbonaceous crystallinity changes during aerogel capture will facilitate conclusions about the structure, chemistry and diversity of carbonaceous matter in comet 81P/Wild 2. For example, Fig. 4 shows Raman measurements of Stardust particles from a large number of particles. Grey circles outline values collected for specific tracks and particles. Particle F13B "Don" consistently exhibits poorly crystallized carbonaceous materials, well removed from spectral values that indicate strong shock processing in coals, which indicates that this particle retains much or all of its cometary structure and was relatively unaffected during capture. This is consistent with a moderate D/H recorded for this particle (McKeegan 2006). By contrast, Raman G band values for particle 35, 25 cover a range of values near the trendline midpoint and so may represent a strongly capture-altered particle. Particle 41,11 exhibits a range of values along the trendline that may indicate locally varying degrees of capture alteration or surviving heterogeneity in the cometary particle. One sample presented here, particle 81,1, is composed of crystalline graphite. The example of PSOC 1468 shows that some material can be graphitized upon capture, which complicates the simple explanation that 81,1 is a relict graphite grain. Additional study is necessary to discern the origin of this grain, which must have attained its present form in a high-temperature process.

CONCLUSIONS

It is important to stress that the measurements presented here are confined to the test particle exteriors, and while this may be representative of the entire body for grains of small size (micrometer), further work is necessary to determine the extent of alteration of the bulk material in larger grains and especially within mineral-dominated particles. While aerogel embedded particle surfaces underwent extreme alteration in structure, the overall change was more homogenizing than randomizing. Graphite particles were severely amorphized by capture and resulted in the most poorly ordered final material of those tested, probably due to the relatively low toughness of crystalline graphite. Coals of varying composition and structure produced Raman spectra of remarkable similarity upon capture. Captured particles (excepting graphite powder) exhibit G-band center and width values of 1593.3 ± 4.2 and 75.6 ± 13.2, respectively. This means that interpretation of Stardust particles featuring this range of values must include consideration of the possibility that the particle was extensively altered during capture. Figure 4 shows examples of two Stardust particles that clearly do not indicate gross capture alteration effects (F13B and 41,11), while a third (35, 25) may feature capture alteration of its carbonaceous material.

On capture, graphitic materials in direct contact with aerogel tend to amorphize while relatively disordered, heteroatom-rich materials apparently undergo devolatilization and crystallization processing. It would be useful to measure the apparent devolatilization directly, but it can be inferred through the pronounced crystalline ordering on capture. A competing hypothesis is that this ordering arises from shear strain at the sample surface during capture and may not require significant devolatilization. While the exact mechanisms at work require further investigation to constrain, a general trend in capture alteration for comparison to Stardust particles is shown here. Trends also arise in multiple Raman analyses of individual particles that provide much richer interpretation of the original particle's composition and structure than can be derived from a single spectrum.

One coal sample, hvCb DECS 24, completely disassociated during capture. The possibility exists that this is because of the high organic sulfur content of this material. If this hypothesis proves to be true, then Stardust particles may be biased against preservation of sulfur-rich carbonaceous materials.

An important caveat to interpretation of carbonaceous materials on the basis of their crystalline ordering arises from this data. Carbonaceous materials that feature a weakly organized structure are not necessarily "primitive" due to shock processing during aerogel capture, as we have demonstrated in alteration of the powdered graphite sample to highly amorphous material. Interpretation of amorphous carbon structure in Stardust carbon should take into account

the possibility of disruption during capture. Also, a single example exists of apparent graphitization of a captured particle (Fig. 3, PSOC 1468 in homogenous aerogel) that indicates that this can occasionally occur for carbonaceous material in direct contact with molten aerogel.

Acknowledgments—M. Fries gratefully acknowledges the support of the NASA SSAP program, grant number 06-SSAP-0003. M. J. Burchell thanks STFC (UK) for funding the light gas gun work.

Editorial Handling—Dr. John Bradley

REFERENCES

ASTM Standard D3172-07a. 2007. Standard practice for proximate analysis of coal and coke. ASTM International, West Conshohocken, PA, 2007, DOI: 10.1520/D3172-07a.

Berger E., Keller L., Joswiak D., Matrajt G., and Lauretta D. 2008. Low-temperature sulfides in Stardust: TEM analysis of a sphalerite/pyrrhotite assemblage from track 7 (abstract #5298). *Meteoritics & Planetary Science* 43:A24.

Beyssac O., Brunet F., Petitet J.-P., Goffe B., and Rouzaud J.-N. 2003. Experimental study of the microtextural and structural transformations of carbonaceous materials under pressure and temperature. *European Journal of Mineralogy* 15:937–951.

Brownlee D., Tsou P., Aléon J., Alexander C. M. O., Araki T., Bajt S., Baratta G. A., Bastien R., Bland P., Bleuet P., Borg J., Bradley J. P., Brearley A., Brenker F., Brennan S., Bridges J. C., Browning N. D., Brucato J. R., Bullock E., Burchell M. J., Busemann H., Butterworth A., Chaussidon M., Cheuvront A., Chi M. F., Cintala M. J., Clark B. C., Clemett S. J., Cody G., Colangeli L., Cooper G., Cordier P., Daghlian C., Dai Z. R., D'Hendecourt L., Djouadi Z., Dominguez G., Duxbury T., Dworkin J. P., Ebel D. S., Economou T. E., Fakra S., Fairey S. A. J., Fallon S., Ferrini G., Ferroir T., Fleckenstein H., Floss C., Flynn G., Franchi I. A., Fries M., Gainsforth Z., Gallien J. P., Genge M., Gilles M. K., Gillet P., Gilmour J., Glavin D. P., Gounelle M., Grady M. M., Graham G. A., Grant P. G., Green S. F., Grossemy F., Grossman L., Grossman J. N., Guan Y., Hagiya K., Harvey R., Heck P., Herzog G. F., Hoppe P., Hörz F., Huth J., Hutcheon I. D., Ignatyev K., Ishii H., Ito M., Jacob D., Jacobsen C., Jacobsen S., Jones S., Joswiak D., Jurewicz A., Kearsley A. T., Keller L. P., Khodja H., Kilcoyne A. L. D., Kissel J., Krot A., Langenhorst F., Lanzirotti A., Le L., Leshin L. A., Leitner J., Lemelle L., Leroux H., Liu M. C., Luening K., Lyon I. 2006. Comet 81P/Wild 2 under a microscope. *Science* 314:1711–1716.

Burchell M. J., Cole M. J., McDonnell J. A. M., and Zarnecki J. C. 1999. Hypervelocity impact studies using the 2 MV Van de Graaff dust accelerator and two stage light gas gun of the University of Kent at Canterbury. *Measurement Science & Technology* 10:41–50.

Burchell M. J., Creighton J. A., Cole M. J., Mann J., and Kearsley A. T. 2001. Capture of particles in hypervelocity impacts in aerogel. *Meteoritics & Planetary Science* 36:209–221.

Burchell M. J., Creighton J. A., and Kearsley A. T. 2004. Identification of organic particles via Raman techniques after capture in hypervelocity impacts on aerogel. *Journal of Raman Spectroscopy* 35:249–253.

Burchell M. J., Graham G., and Kearsley A. 2006a. Cosmic dust collection in aerogel. *Annual Reviews of Earth and Planetary Science* 34:385–418.

Burchell M. J., Mann J., Creighton J. A., Kearsley A. T., Graham G., and Franchi I. A. 2006b. Identification of minerals and meteoritic materials via Raman techniques after capture in hypervelocity impacts on aerogel. *Meteoritics & Planetary Science* 41:217–232.

Burchell M., Fairey S., Foster N., and Cole M. 2009. Hypervelocity capture of particles in aerogel: Dependence on aerogel properties. *Planetary and Space Science* 57:58–70.

Cody G., Alexander C. M. O'D., Yabuta H., Kilcoyne A. L. D., Araki T., Ade H., Dera P., Fogel M., Militzer B., and Mysen B. O. 2008. Organic thermometry for chondritic parent bodies. *Earth and Planetary Science Letters* 272:446–455.

Cody G., Ade H., Alexander C. M. O'D., Araki T., Butterworth A., Fleckenstein H., Flynn G., Gilles M., Jacobsen C., Kilcoyne A. L. D., Messenger K., Sandford S., Tyliszczak T., Westphal A., Wirick S., and Yabuta H. 2008. Quantitative organic and light-element analysis of comet 81P/Wild 2 particles using C-, N-, and O- μ-XANES. *Meteoritics & Planetary Science* 43:353–365.

Crespo D. and Pradell T. 1996. Evaluation of time-dependent grain-size populations for nucleation and growth kinetics. *Physical Review B* 54:3101–3109.

Fischbach D. 1963. Kinetics of graphitization of a petroleum coke. *Nature* 200:1281–1283.

Flynn G. and The Stardust Composition Team. 1996. Stardust: Composition of Wild 2 samples. 36th COSPAR Scientific Assembly, Abstract #579.

Foster N. J., Burchell M. J., Creighton A. J., and Kearsley A. T. 2007. Does capture in aerogel change carbonaceous Raman D and G bands? (abstract #1647). 38th Lunar and Planetary Science Conference. CD-ROM.

Greenberg J. 1998. Making a comet nucleus. *Astronomy and Astrophysics* 330:375–380.

De Gregorio B., Stroud R., Nittler L., and Cody G. 2009. Variety of organic matter in Stardust return samples from comet 81P/Wild 2 (abstract #2260). 40th Lunar and Planetary Science Conference. CD-ROM.

Hoppe P., Heck P., Hörz F., Huth J., Marhas K., Messenger K., Snead C., and Westphal A. NanoSIMS studies of dust projectile shots into Stardust-type aerogel and aluminum foils (abstract #1546). 37th Lunar and Planetary Science Conference. CD-ROM.

Hörz F., Cintala M. J., See T. H., and Nakamura-Messenger K. 2008. Impact experiments with Al_2O_3 projectiles into aerogel (abstract #1391). 39th Lunar and Planetary Science Conference. CD-ROM.

Hörz F., Cintala M. J., See T. H., and Nakamura-Messenger K. 2009. Penetration tracks in aerogel produced by Al_2O_3 spheres. *Meteoritics & Planetary Science* 44: 1243–1264.

Irvine W. 1998. Extraterrestrial organic matter: A review. *Origins of Life and Evolution of Biospheres* 28:4–6, 365–383.

Jones M. J. 2007. A method for producing gradient density aerogel. *Journal of Sol-Gel Science and Technology* 44:255–258.

Keller L. P., Bajt S., Baratta G. A., Borg J., Bradley J. P., Brownlee D. E., Busemann H., Brucato J. R., Burchell M., Colangeli L., D'Hendecourt L., Djouadi Z., Ferrini G., Flynn G., Franchi I. A., Fries M., Grady M. M., Graham G. A., Grossemy F., Kearsley A., Matrajt G., Nakamura-Messenger K., Mennella V., Nittler L., Palumbo M. E., Stadermann F. J., Tsou P., Rotundi A., Sandford S. A., Snead C., Steele A., Wooden D., and Zolensky M. 2006. Infrared spectroscopy of comet 81P/Wild 2 samples returned by Stardust. *Science* 314:1728–1731.

Matrajt G., Ito M., Wirick S., Messenger S., Brownlee D., Joswiak D., Flynn G., Brownlee D., Tsou P., Aléon J., Alexander C. M. O'D., Araki T., Bajt S., Baratta G. A., Bastien R., Bland P., Bleuet P., Borg J., Bradley J. P., Brearley A., Brenker F., Brennan S., Bridges J. C., Browning N., Brucato J. R.,

Brucato H., Bullock E., Burchell M. J., Busemann H., Butterworth A., Chaussidon M., Cheuvront A., Chi M., Cintala M. J, Clark B. C., Clemett S. J., Cody G., Colangeli L., Cooper G., Sandford S., Snead C., and Westphal A. 2008. Carbon investigation of two Stardust particles: A TEM, NanoSIMS, and XANES study. *Meteoritics & Planetary Science* 43:315–334.

Matthews M., Pimenta M., Dresselhaus G., Dresselhaus M., and Endo M. 1999. Origin of dispersive effects of the Raman D band in carbon materials. *Physical Review B* 59(10):R6585–R6588.

McKeegan K. D., Aleon J., Bradley J., Brownlee D., Busemann H., Butterworth A., Chaussidon M., Fallon S., Floss C., Gilmour J., Gounelle M., Graham G., Guan Y. B., Heck P. R., Hoppe P., Hutcheon I. D., Huth J., Ishii H., Ito M., Jacobsen S. B., Kearsley A., Leshin L. A., Liu M. C., Lyon I., Marhas K., Marty B., Matrajt G., Meibom A., Messenger S., Mostefaoui S., Mukhopadhyay S., Nakamura-Messenger K., Nittler L., Palma R., Pepin R. O., Papanastassiou D. A., Robert F., Schlutter D., Snead C. J., Stadermann F. J., Stroud R., Tsou P., Westphal A., Young E. D., Ziegler K., Zimmermann L., and Zinner E. 2006. Isotopic compositions of cometary matter returned by Stardust. *Science* 314:1724–1728.

Murty H., Biederman D., and Heintz E. 1969. Kinetics of graphitization—I. Activation energies. *Carbon* 7:667–681.

Murty H., Biederman D., and Heintz E. 1969. Kinetics of graphitization—II. Pre-exponential factors. *Carbon* 7:683–688.

Nakamura-Messenger K., Messenger S., Keller L., Clemmett S., and Zolensky M. 2006. Organic globules in the Tagish Lake meteorite: Remnants of the protosolar disk. *Science* 314:1439–1442.

Noguchi T., Nakamura T., Okydaira K., Yano H., Sugita S., and Burchell M. 2007. Thermal alteration of hydrated minerals during hypervelocity capture to silica aerogel at the flyby speed of Stardust. *Meteoritics & Planetary Science* 42:357–372.

Roskosz M., Leroux H., and Watson H. C. 2008. 1827. Thermal history, partial preservation and sampling bias recorded by Stardust cometary grains during their capture. *Earth and Planetary Science Letters* 273:195–202.

Rotundi A., Baratta G. A., Borg J., Brucato J. R., Busemann H., Colangeli L., D'Hendecourt L., Djouadi Z., Ferrini G., Franchi I. A., Fries M., Grossemy F., Keller L. P., Mennella V., Nakamura K., Nittler L. R., Palumbo M. E., Sandford S. A., Steele A., and Wopenka B. 2008. Combined micro-Raman, micro-infrared, and field emission scanning electron microscopy analyses of comet 81P/Wild 2 particles collected by Stardust. *Meteoritics & Planetary Science* 43:367–397.

Sandford S. A., Aléon J., Alexander C. M. O., Araki T., Bajt S., Baratta G. A., Borg J., Bradley J. P., Brownlee D. E., Brucato J. R., Burchell M. J., Busemann H., Butterworth A., Clemett S. J., Cody G., Colangeli L., Cooper G., D'Hendecourt L., Djouadi Z., Dworkin J. P., Ferrini G., Fleckenstein H., Flynn G. J., Franchi I. A., Fries M., Gilles M. K., Glavin D. P., Gounelle M., Grossemy F., Jacobsen C., Keller L. P., Kilcoyne A. L. D., Leitner J., Matrajt G., Meibom A., Mennella V., Mostefaoui S., Nittler L. R., Palumbo M. E., Papanastassiou D. A., Robert F., Rotundi A., Snead C. J., Spencer M. K., Stadermann F. J., Steele A., Stephan T., Tsou P., Tyliszczak T., Westphal A. J., Wirick S., Wopenka B., Yabuta H., Zare R. N., and Zolensky M. E. 2006. Organics captured from comet 81P/Wild 2 by the Stardust spacecraft. *Science* 314:1720–1724.

Sood A., Gupta R., and Asher S. 2001. Origin of the unusual dependence of Raman D band on excitation wavelength in graphite-like materials. *Journal of Applied Physics* 90:4494–4497.

Trigo-Rodríguez J. M., Dominguez G., Burchell M. J., Hörz F., and Llorca J. 2008. Bulbous tracks arising from hypervelocity capture in aerogel. *Meteoritics & Planetary Science* 43:75–86.

Tsou P., Brownlee D. E., Sandford S. A, Hörz F., and Zolensky M. E. 2003. Wild 2 and interstellar sample collection and Earth return. *Journal of Geophysical Research* 108(E10), 8113:1–21.

Tuinstra F. and Koenig J. 1970. Raman spectrum of graphite. *Journal of Chemical Physics* 53:1126–1130.

Wopenka B., Matrajt G., Bajt S., Joswiak D., and Brownlee D. 2008. Carbonaceous phases characterized in two individual Stardust particles: FTIR and Raman spectra of Febo and Ada (abstract #1827). 39th Lunar and Planetary Science Conference. CD-ROM.